Experimental Output Regulation for a Nonlinear Benchmark System

Alexey Pavlov, Bart Janssen, Nathan van de Wouw, and Henk Nijmeijer, *Fellow, IEEE*

***Abstract*—Research on the nonlinear output regulation problem is mainly focused on theoretical developments and studies on simulation level. In this brief, we present experimental results on the local output regulation problem for a nonlinear benchmark mechanical system, the so-called translational oscillator with a rotational actuator system. The presented results show the effectiveness of the nonlinear output regulation theory in practice. As follows from the conducted experiments, issues such as the convergence rate, stability, and performance robustness with respect to (non) parametric uncertainties, the size of the region of attraction, and actuator saturation should be accounted for in tuning the controller gains. This design problem has not been addressed in the existing literature on the nonlinear output regulation problem and it, therefore, raises a new direction for research crucial to the future application of output regulation theory in practice.**

***Index Terms*—Disturbance rejection, experimental output regulation, nonlinear mechanical systems, output regulation, translational oscillator with a rotational actuator (TORA) system.**

I. Introduction

THE OUTPUT regulation problem is one of the most important problems in control theory. It includes the problems of tracking reference signals and rejecting disturbances generated by an external autonomous system (exosystem). For linear systems, this problem was thoroughly investigated in the 1970s, see, e.g., [1] and [2]. For nonlinear systems, intensive research on the output regulation problem started with [3] and [4], which provided solutions to the local output regulation problem for general nonlinear systems. These papers were followed by a number of results dealing with different aspects of the output regulation problem for nonlinear systems: approximate, robust, and adaptive output regulation. For references on theoretical developments on the subject, the reader is referred to [5] and monographs [6]–[9]. For a number of nonlinear mechanical systems, the output regulation problem has been studied in [10]–[14] and in the recent monograph [7]. Despite the significant interest in this problem, most of the known results are theoretical with only a few papers aiming at experimental validation of the proposed solutions [15], [16]. In [15], the output regulation theory for nonlinear systems has been applied to the problem of fault tolerant control of induction motors. For mechanical systems, to the best of our knowledge, there is only one paper [16] describing an experimental setup for testing controllers for the nonlinear output regulation problem. Yet, that paper contains experimental results only for the case of controllers designed on the basis of a linearized model of the system. Experiments with controllers designed on the basis of the *nonlinear* output regulation theory (which dominate in recent publications) are still missing in the literature. This fact motivates our studies in experimental output regulation of nonlinear systems.

This brief aims to fill in the gap between theory and experiments in the field of output regulation for nonlinear systems. We present results on experimental output regulation for the so-called translational oscillator with a rotational actuator (TORA) system. This system is a nonlinear benchmark mechanical system used for testing many nonlinear control techniques, see, e.g., [17]–[19]. On a theoretical level, the local output regulation problem for the TORA system has been previously considered in [12], [20], and [21].

The reason for the experimental study presented in this brief is twofold. The first reason is to check whether the controllers from the nonlinear output regulation theory are applicable in an experimental setting in the presence of disturbances and modeling uncertainties, which are inevitable in practice. The second reason is to identify problems or difficulties that arise at the stage of application of output regulation controllers. These practical problems, not being fully investigated in the existing theory, give rise to future research directions in the theory on the nonlinear output regulation problem. As such, the results presented in this brief should be considered as the first steps in experimental output regulation for nonlinear systems.

This brief is organized as follows. In Section II, we describe the TORA system and state a local disturbance rejection problem for this system. This problem is a particular case of the local nonlinear output regulation problem. In Section III, a controller solving this disturbance rejection problem is presented. The experimental setup is described in Section IV. In Section V, we present and discuss experimental results. Section VI contains the conclusion. This brief is an extended variant of [22].

Manuscript received April 18, 2005; revised February 8, 2006. This work was supported in part by The Netherlands Organization for Scientific Research NWO and by the Research Council of Norway under the Strategic University Program CM-in-MC.

A. Pavlov is with the Department of Engineering Cybernetics, Norwegian University of Science and Technology, Trondheim NO-7491, Norway (e-mail: alexey.pavlov@itk.ntnu.no).

B. Janssen is with DTI–Advanced Technologies, 5616 TB Eindhoven, The Netherlands (email: b.r.a.janssen@gmail.com).

N. van de Wouw, and H. Nijmeijer are with the Department of Mechanical Engineering, Eindhoven University of Technology, 5600 MB Eindhoven, The Netherlands (e-mail: n.v.d.wouw@tue.nl; h.nijmeijer@tue.nl).

Digital Object Identifier 10.1109/TCST.2006.890294

II. Output Regulation of the TORA System

Consider the so-called TORA-system, which is shown in Fig. 1. This system consists of a cart of mass M that is attached to a wall with a spring of stiffness k. The cart is excited by a disturbance force F_d. In the center of the cart there is a rotating arm of mass m. The center of mass of the arm CM is located at a distance l from the rotational axis and the arm has an inertia J with respect to this axis. The arm is actuated by a control torque T_u. The cart and the arm move in the horizontal plane and,

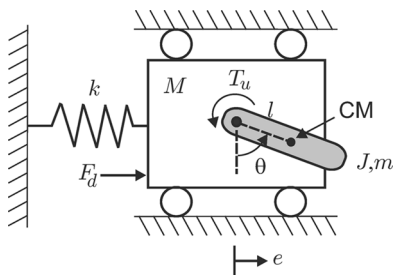

Fig. 1. TORA system.

therefore, gravity effects are omitted. The horizontal displacement of the cart is denoted by e and the angular displacement of the arm is denoted by θ.

The control problem is to find a control law for the torque T_u such that the horizontal displacement e tends to zero in presence of a harmonic disturbance force F_d. The frequency of the disturbance force is known in advance and can be used in the controller design, while the amplitude and phase of F_d may vary. This is a particular case of the local output regulation problem, see, e.g., [6] and [23].

Historically, the output regulation problem was mostly considered for the case of harmonic excitations. From the practical point of view, this can be justified by the fact that in many problems disturbances may have several dominating harmonics. In addition to that, it is common in engineering practice to first consider the case of harmonic disturbances before reverting to general (e.g., stochastic) disturbance models. Disturbances in practice mostly have several dominating harmonics. A variant of the previously stated disturbance rejection problem for the case of a disturbance with multiple, but finite number of harmonics, even though these harmonics may be commensurate, does not pose additional difficulties in the controller design. Yet considering such a case would add extra technicalities. To avoid these unnecessary technicalities, we consider the disturbance rejection problem for the case of the disturbance with one harmonic.

In Section III, we design a controller solving the previously stated disturbance rejection problem locally, i.e., for sufficiently small initial conditions $e(0)$, $\dot{e}(0)$, $\theta(0)$, and $\dot{\theta}(0)$ and for disturbances with sufficiently small amplitudes. This controller will be designed based on the theory of local output regulation for nonlinear systems. In this approach, the region of initial conditions and the magnitude of the admissible disturbances for which output regulation is attained depends on the chosen controller and, in general, cannot be set in advance. When a controller solving the local output regulation problem is found, the region of admissible initial conditions and the magnitude of the admissible disturbances can be estimated, see, e.g., [20]. Since in this brief we focus on experimental validation of output regulation controllers, we will not address this estimation problem.

III. Controller Design for the TORA System

In this section, we design a simple controller for the disturbance rejection problem considered in Section II. The equations of motion for the TORA system are given by [17]

$$\begin{aligned} \bar{M}\ddot{e} + ml(\ddot{\theta}\cos\theta - \dot{\theta}^2\sin\theta) + ke &= F_d \\ J\ddot{\theta} + ml\ddot{e}\cos\theta &= T_u \end{aligned} \tag{1}$$

where $\bar{M} := M + m$. The disturbance force F_d is generated by the linear exosystem

$$\dot{w} = Sw \quad F_d = w_1 \tag{2}$$

where

$$w = \begin{bmatrix} w_1 \\ w_2 \end{bmatrix} \quad S := \begin{bmatrix} 0 & \omega \\ -\omega & 0 \end{bmatrix}$$

and ω is the oscillation frequency. The initial conditions of the exosystem (2) determine the amplitude and phase of the excitation. The control problem is to asymptotically regulate $e(t)$ to zero for all sufficiently small initial conditions of the closed-loop system and for all sufficiently small initial conditions of the exosystem and at the same time to guarantee that for $F_d = 0$ the closed-loop system has an asymptotically stable linearization at the origin. For simplicity, in this experimental study, we will deal only with state-feedback controllers solving this local output regulation problem. For this reason, it is assumed that e, $\dot{e}$, θ, $\dot{\theta}$, w_1, and w_2 are measured and all parameters of the system are known. Notice that this output regulation problem also admits a solution for the case of only e available for measurements, see, e.g., [12]. Yet such an output feedback controller would add more complexity and make the experimental analysis presented in this brief less transparent.

In order to solve this output regulation problem we, first, rewrite system (1) in the following form:

$$\begin{aligned} x &= f(x) + g_u(x)T_u + g_d(x)F_d \\ e &= x_1 \\ F_d &= w_1 \end{aligned} \tag{3}$$

where $x := [e, \dot{e}, \theta, \dot{\theta}]^T$ is the state of system (1) and

$$f(x) := \frac{1}{\Delta}\begin{bmatrix} \Delta x_2 \\ mlJx_4^2\sin x_3 - kJx_1 \\ \Delta x_4 \\ -m^2l^2x_4^2\cos x_3\sin x_3 + klmx_1\cos x_3 \end{bmatrix}$$

$$g_u(x) := \frac{1}{\Delta}\begin{bmatrix} 0 \\ -ml\cos x_3 \\ 0 \\ \bar{M} \end{bmatrix}$$

$$g_d(x) := \frac{1}{\Delta}\begin{bmatrix} 0 \\ J \\ 0 \\ -ml\cos x_3 \end{bmatrix}$$

and $\Delta := \bar{M}J - m^2l^2\cos^2 x_3$. Notice that since $\bar{M} > m$ and $J > ml^2$, we obtain $\Delta(x) \geq \bar{M}J - m^2l^2 > 0$ for all $x \in \mathbb{R}^4$.

Following [3] and [6], we seek a controller solving the local output regulation problem in the form

$$T_u = c(w) + K\left(x - \pi(w)\right) \tag{4}$$

where the matrix K is such that for $w = 0$ the closed-loop system (3) and (4) has an asymptoti-

cally stable linearization at the origin. The mappings $\pi(w) := [\pi_1(w), \pi_2(w), \pi_3(w), \pi_4(w)]^T$ and $c(w)$, with $\pi(0) = 0$ and $c(0) = 0$, are C^1 mappings which are defined in a neighborhood of the origin $w = 0$ and satisfy the so-called regulator equations [3], [6]

$$\begin{aligned} \frac{\partial \pi}{\partial w} Sw &= f(\pi(w)) + g_u(\pi(w))\, c(w) + g_d(\pi(w))\, w_1 \\ \pi_1(w) &= 0. \end{aligned} \tag{5}$$

The solutions to the regulator equations have the following meaning. For any sufficiently small solution of the exosystem $w(t)$, for the disturbance force $F_d(t) = w_1(t)$ and controller action $T_u(t) = c(w(t))$, the function $x(t) = \pi(w(t))$ is a solution of system (3) [or, equivalently, of system (1)] and along this solution the displacement $e(t)$ equals zero. By substitution, one can easily check that the mappings

$$\pi_1(w) = 0$$
$$\pi_2(w) = 0$$
$$\pi_3(w) = -\arcsin\left(\frac{w_1}{ml\omega^2}\right) \tag{6}$$
$$\pi_4(w) = -\frac{\omega w_2}{(m^2 l^2 \omega^4 - w_1^2)^{1/2}} \tag{7}$$
$$c(w) = \frac{\omega^2 w_1 \left(m^2 l^2 \omega^4 - w_1^2 - w_2^2\right) J}{(m^2 l^2 \omega^4 - w_1^2)^{3/2}} \tag{8}$$

satisfy the regulator equations.

The requirement on the matrix K is equivalent to the requirement that $A + BK$ is a Hurwitz matrix, where the matrices

$$A := \begin{bmatrix} 0 & 1 & 0 & 0 \\ -\frac{kJ}{\bar{M}J - m^2 l^2} & 0 & 0 & 0 \\ 0 & 0 & 0 & 1 \\ \frac{kml}{\bar{M}J - m^2 l^2} & 0 & 0 & 0 \end{bmatrix} \quad B := \begin{bmatrix} 0 \\ -\frac{ml}{\bar{M}J - m^2 l^2} \\ 0 \\ \frac{\bar{M}}{\bar{M}J - m^2 l^2} \end{bmatrix}$$

follow from the linearization of system (3) at the origin with $F_d = 0$ and T_u viewed as input. One can easily check that the inequality $\bar{M}J - m^2 l^2 > 0$, which is satisfied, implies controllability of the pair (A, B). Hence, we can always choose a matrix K such that $A + BK$ is Hurwitz. As follows from [3] and [6], controller (4) solves the local output regulation problem. This controller admits some freedom in the choice of the matrix K. This freedom can be used, for example, in tuning the controller to obtain desirable performance and robustness properties of the closed-loop system. Controller (4) is implemented in the experimental setup described in Section IV.

IV. Experimental Setup

The experimental setup has been constructed by adapting an existing X–Y positioning system (the H-bridge setup) in the Dynamics and Control Technology Laboratory, Eindhoven University of Technology. The setup is shown in Fig. 2.

A. Setup Description

The adapted H-bridge setup is schematically shown in Fig. 3. It consists of the following components. The two parallel axes

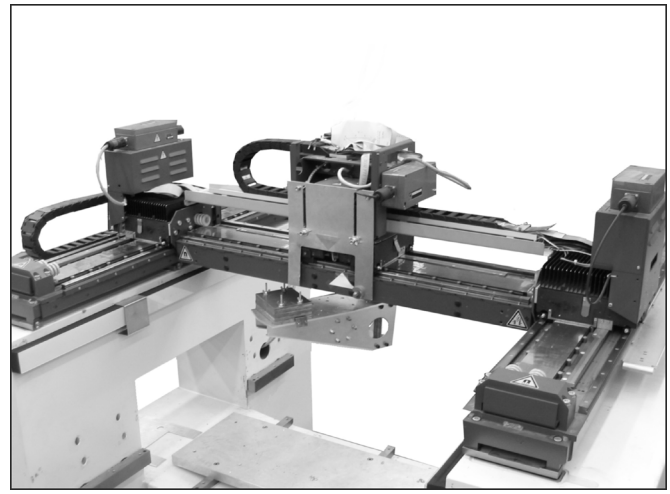

Fig. 2. Adapted H-bridge setup.

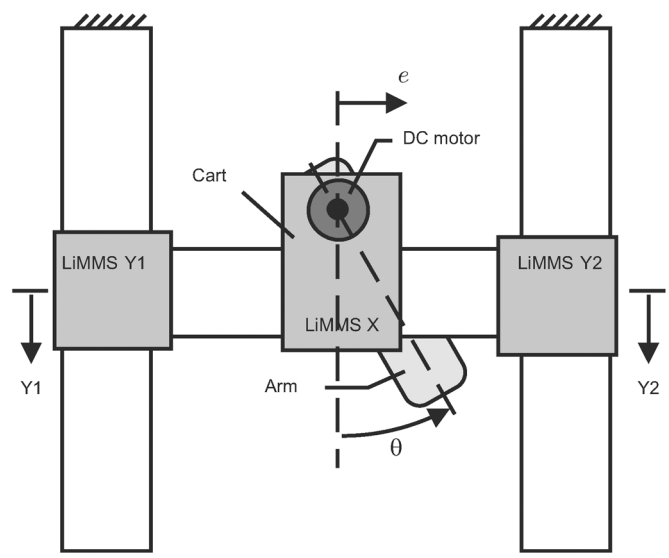

Fig. 3. Adapted H-bridge setup scheme (top view).

$Y1$ and $Y2$ are equipped with linear magnetic motor systems LiMMS $Y1$ and LiMMS $Y2$ that can move along their axes. These two carriages support the X-axis. Along the X-axis moves the X-LiMMS carriage, which we will refer to as the cart. In all experiments that are performed on this setup, the $Y1$ and $Y2$ carriages are controlled to maintain a fixed position with a low-level proportional–integral–differential (PID) controller. The bandwidth of this controller is chosen such that the closed-loop dynamics of the $Y1$ and $Y2$ carriages does not affect the low-frequency dynamics of the cart motion along the X-axis. This motion is of primary interest in the experiments performed on the setup. Therefore, in the sequel, we assume that the $Y1$ and $Y2$ carriages stand still, i.e., the X-axis is fixed.

The mass of the cart moving along the X-axis is M [kg]. The displacement of the cart e [m] is measured using a linear incremental encoder with a 1-μm resolution. The force applied to the cart by the linear motor is proportional to the voltage control signal u_F which is fed to the linear motor through a proportional amplifier, i.e., $F = \kappa_F u_F$. The constant κ_F has the value of 74.4 N/V ([24]). In addition to the actuating force,

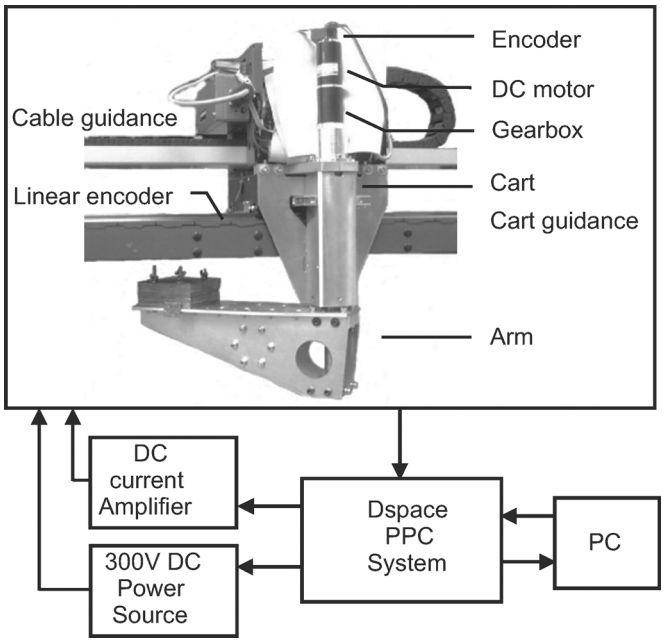

Fig. 4. Adapted H-bridge setup: rear view and connection scheme.

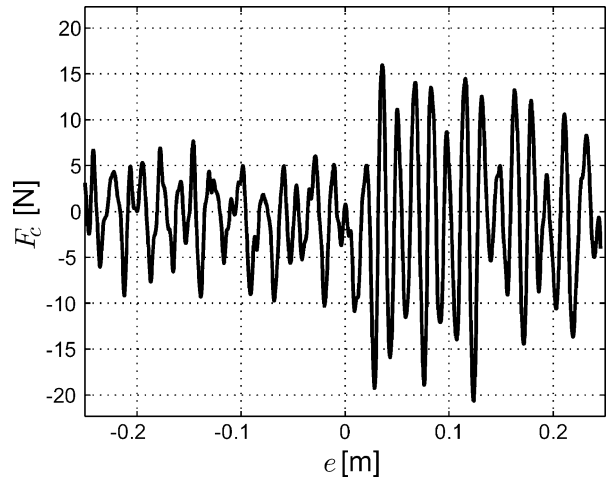

Fig. 5. Identified cogging force $F_c(e)$.

a friction force $F_f = F_f(\dot{e})$ is present in the roller bearings of the cart. This friction force consists of the Coulomb and viscous friction forces and, therefore, depends on the cart velocity $\dot{e}$. Moreover, there is a position dependent cogging force $F_c = F_c(e)$. This cogging force is caused by the interaction of the permanent magnets in the X-axis stator base and the iron-core coils of the electromagnets in the cart (see [24] for details). We assume that the friction force depends only on the cart velocity, i.e., $F_f = F_f(\dot{e})$, and the cogging force depends only on the position of the cart, i.e., $F_c = F_c(e)$. This assumption, although being a simplification of reality, helps us with dealing with these two forces.

In order to transform the H-bridge into a TORA system, additional hardware has been added to the cart, see Fig. 4. A vertical shaft supported by a set of deep-groove and angular contact ball bearings is attached to the back of the cart, thus, forming a rotational joint. An arm of mass m kg is attached to the lower end of the shaft. The center of mass of the arm is located at the distance l m from the shaft center line. A 48-V, 150-W dc motor (Maxon RE40), fitted with a ceramic planetary gearhead, with the gear ratio $g_r = 113$, drives the shaft via an adapted flexible coupling. The angular position of the motor shaft is measured by a rotational incremental encoder with a quadrature decoded resolution of 0.18°. Taking into account the gear ratio, this results in an approximate resolution 0.0016° of the angular position θ of the rotating arm. The total inertia of all rotating parts (the arm, shaft, coupling, bearings, gearhead, and motor) with respect to the shaft is J kg $\cdot$ m^2. Due to the friction in the motor, gearhead, and ball bearings of the shaft, an additional friction torque $T_f = T_f(\dot{\theta})$ acts on the arm. This friction torque consists of the Coulomb friction torque and the viscous friction torque and, therefore, it depends on the angular velocity $\dot{\theta}$. The assumption that the friction torque depends only on the angular velocity is a simplification of reality, since, the friction in the gearhead also depends on the torque. The torque T generated by the dc motor is proportional to the current i A fed to the motor, i.e., $T = \kappa_T i$, where $\kappa_T = 60.3$ mN $\cdot$ m/A is the motor constant. The current i is generated by an analog current amplifier. It is proportional to the voltage control signal u_T fed to the amplifier, i.e., $i = \kappa_A u_T$, where $\kappa_A = 1.6$ A/V is the amplifier constant. The dynamics of the motor and the amplifier are much faster than the dynamics of the mechanical part of the setup, which are predominantly low-frequent in the performed experiments. Therefore, in our experiments, the motor and the amplifier dynamics can be neglected and we can assume that there is a static relation between the voltage control signal u_T and the motor torque T, i.e., $T = g_r \kappa_T \kappa_A u_T$.

Taking into account all the active forces and torques, we use the equations of Lagrange for the setup consisting of the cart moving along the fixed X-axis and the (horizontally) rotating arm attached to the cart. The corresponding model has the following form:

$$\begin{aligned} \bar{M}\ddot{e} + ml(\ddot{\theta}\cos\theta - \dot{\theta}^2\sin\theta) &= F - F_f(\dot{e}) + F_c(e) \\ J\ddot{\theta} + ml\ddot{e}\cos\theta &= T - T_f(\dot{\theta}) \end{aligned} \tag{9}$$

where $\bar{M} := M + m$, the actuator force acting on the cart equals $F = \kappa_F u_F$ and the actuator torque acting on the arm equals $T = g_r \kappa_T \kappa_A u_T$, where u_F and u_T are the actuating signals for the cart and for the arm, respectively.

The cogging force $F_c(e)$ and the friction force $F_f(\dot{e})$ have been identified using dedicated experiments [24], see Figs. 5 and 6, respectively. The friction torque $T_f(\dot{e})$ has been identified using constant angular velocity tests. The resulting graph is given in Fig. 7.

Initial estimates of the inertia J and the product ml are computed from the computer-aided design (CAD) drawings, material data, and specifications of the motor and gearhead. These estimates are $J = 0.5405$ kg $\cdot$ m^2 and $ml = 1.2514$ kg $\cdot$ m. The estimate of the cart mass $\bar{M} = 20.965$ kg is obtained by weighing additional hardware mounted on the cart and summing this mass with the mass of the cart itself (which is not detachable from the setup and cannot be weighed) identified in [24]. These estimates will be used as a starting point to obtain more accurate estimates based on closed-loop experiments.

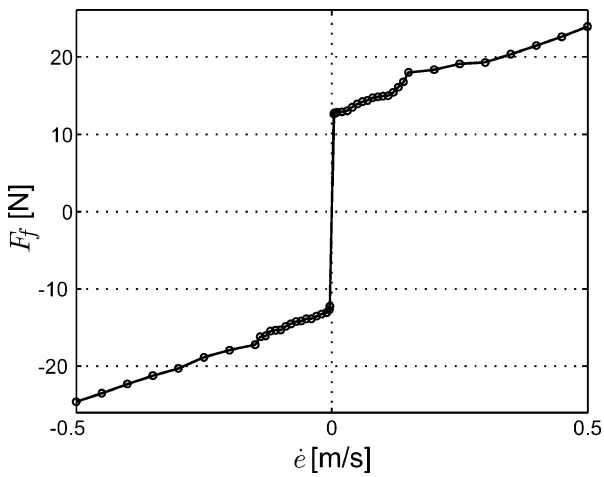

Fig. 6. Identified friction force $F_f(\dot{e})$.

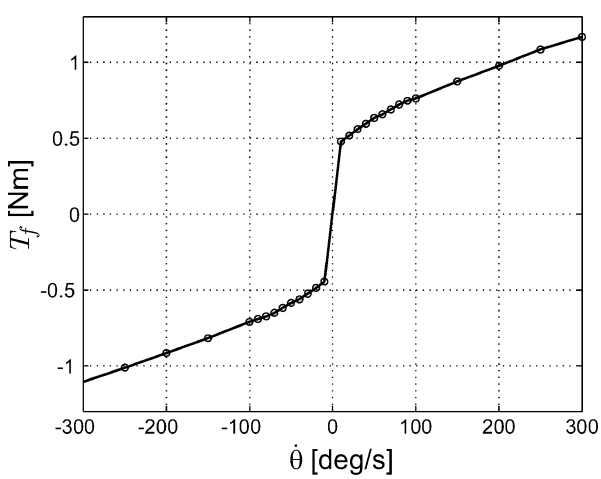

Fig. 7. Identified friction torque $T_f(\dot{\theta})$.

In order to implement the TORA system in the resulting setup, we need to compensate for the friction in the cart and the arm and for the cogging force in the X-axis. Moreover, we need to implement the virtual spring action $-ke$ and the disturbance force F_d along the X-axis. For the cart, this is achieved by the controller

$$u_F = \frac{1}{\kappa_F}\left(\hat{F}_f(\dot{e}) - \hat{F}_c(e) - ke + F_d\right) \tag{10}$$

where $\hat{F}_f(\dot{e})$ and $\hat{F}_c(e)$ are the friction compensation and cogging compensation forces (based on the identified values of these forces, see Figs. 5 and 6), k N/m is the stiffness of the virtual spring (which we can set arbitrarily) and $F_d(t) = w_1(t)$ is the disturbance force acting on the cart. In the experiments performed on the setup, the parameter k is set equal to $k =$ 500 N/m. The exosystem (2), with $w(t) = [w_1(t), w_2(t)]^T$, is integrated in the PC/dSpace-system and the disturbance force $F_d(t) = w_1(t)$ is computed from the obtained solutions.

Next, we need to implement friction compensation in the rotating arm. This is achieved by the controller

$$u_T = \frac{1}{g_r \kappa_T \kappa_A}\left(T_u + \hat{T}_f(\dot{\theta})\right) \tag{11}$$

where $\hat{T}_f(\dot{\theta})$ is the friction compensation torque based on the identified friction torque in the arm, see Fig. 7, and T_u is a new control input.

After implementing the low-level controllers (10), (11), and the exosystem (2), the resulting system takes the form

$$\begin{aligned} \bar{M}\ddot{e} + ml(\ddot{\theta}\cos\theta - \dot{\theta}^2\sin\theta) + ke &= F_d + \varepsilon_F \\ J\ddot{\theta} + ml\ddot{e}\cos\theta &= T_u + \varepsilon_T \end{aligned} \tag{12}$$

where F_d is the disturbance force, T_u is the control torque (new input), and ε_F and ε_T are the residual terms due to nonexact friction and cogging compensation and due to uncertainties in the system parameters. System (12) is now in the form of system (1) (if the residual terms are not taken into account), for which the controller (4) solves the local output regulation problem. This controller requires the values for e and θ, which are measured by the encoders, $\dot{e}$ and $\dot{\theta}$, which are obtained by numerical differentiation and filtering of the measured signals e and θ, and the values of $w_1(t)$ and $w_2(t)$, which are computed in the dSpace-system.

A more detailed description of the experimental setup can be found in [25].

V. Experiments

In this section, we present experimental results performed on the adapted H-bridge setup in closed loop with the controller (4).

A. Parameter Settings

The gain matrix K in controller (4) is set to $K := [29, -1.5, -11, 1.9]$. The eigenvalues of the linearized closed-loop system corresponding to this K and to the initial estimates of the system parameters given in the previous section equal $-1.0313 \pm 5.8493i$ and $-0.9121 \pm 3.8901i$. The choice of the matrix K is determined by several requirements. The first and the third entries in the matrix K, which correspond to the displacement of the cart e and angular position of the arm θ must be large enough to compensate for the residual friction and backlash present in the system. At the same time, the real part of the eigenvalues of the linearized closed-loop system must be less than a certain threshold in order to guarantee fast convergence rates and sufficient robustness properties of the closed-loop system. In theory, for any matrix K such that $A + BK$ is Hurwitz, controller (4) solves the output regulation problem in *some* neighborhood of the origin, i.e., for initial conditions of the closed-loop system and the exosystem being small enough. This neighborhood of admissible initial conditions essentially depends on the choice of K. Thus, our choice of the matrix K must be such that the resulting set of admissible initial conditions is relatively large in order to test this controller in experiments (the problem of estimating this

neighborhood of admissible initial conditions for a system in closed loop with a controller solving the local output regulation problem has been considered in [20], [26], and [27]). Finally, the control signal resulting from the controller with this matrix K must not exceed, in most operating conditions, the bounds imposed by the amplifier and dc motor specifications. Taking these requirements into account, an optimization weighing the previously mentioned performance criteria (based on control engineering judgement) resulted in the matrix K presented before.

In practice, the choice of the gain K is crucial for the performance of the output regulation controller within engineering constraints. At the same time, the problem of tuning the controller gains simultaneously taking into account convergence rate, performance, and stability robustness with respect to parametric and nonparametric uncertainties, the size of the convergence region, and controller saturation has not been considered in the literature on the output regulation problem for nonlinear systems so far. Therefore, this problem stimulates a new direction in future research on the output regulation problem aiming at the enhancements of the applicability of the output regulation theory.

The estimates for the parameters J and ml are tuned based on closed-loop experiments using the output regulation controller (in order to obtain better performance). The new estimates are $\hat{J} = 0.4270$ N $\cdot$ m^2 (21% smaller than the initial estimate) and $\widehat{ml} = 1.3389$ kg $\cdot$ m (7% larger than the initial estimate). These estimates are used in the feedforward part of the output regulation controller in the experiments presented in this brief.

The friction compensation torque in the rotating arm $\hat{T}_f(\dot{\theta})$ is set 1.5 times larger than the identified friction torque $T_f(\dot{\theta})$ given in Fig. 7. Recall that the friction in the gearhead, which is the main contributor to the friction in the arm motion, depends not only on the angular velocity $\dot{\theta}$, but also on the torque applied to the shaft. The higher the torque applied to the shaft is, the larger the friction torque is. Identification of the friction torque has been performed for very low torques (constant velocity experiments), while in the experiments with the TORA controller the torques are much higher. Therefore, the friction compensation torque must be set higher than the identified friction torque $T_f(\dot{\theta})$. The cogging compensation force $\hat{F}(e)$ is set equal to the identified cogging force presented in Fig. 5. The friction compensation force $\hat{F}_f(\dot{e})$ in the cart motion is set to 90% of the identified friction force presented in Fig. 6 to avoid over compensation. Moreover, for a cart velocity $\dot{e}$ of magnitude less than 0.035 m/s, it is set to

$$\hat{F}_f(\dot{e}) := \frac{|\dot{e}|0.90}{0.035} F_f(\dot{e}).$$

In case of exact friction compensation, there will always be over compensation at some velocities due to nonideal friction identification. Such an over compensation in many cases leads to friction-induced limit-cycling, see, e.g., [28], which has been observed in experiments. To avoid this limit-cycling, we opt for 10% friction under compensation. At the same time, friction under compensation makes the equilibrium set in terms of the position of the cart larger. In the experiments presented as follows, this equilibrium set can be easily observed when the cart sticks in a point e_*, which is close, but not equal to zero.

TABLE I
INITIAL CONDITIONS e_0 AND θ_0 USED IN THE EXPERIMENTS

	e_0 [m]	θ_0 [deg]
Experiment # 1	-0.2	20
Experiment # 2	0.2	20
Experiment # 3	0.1	90

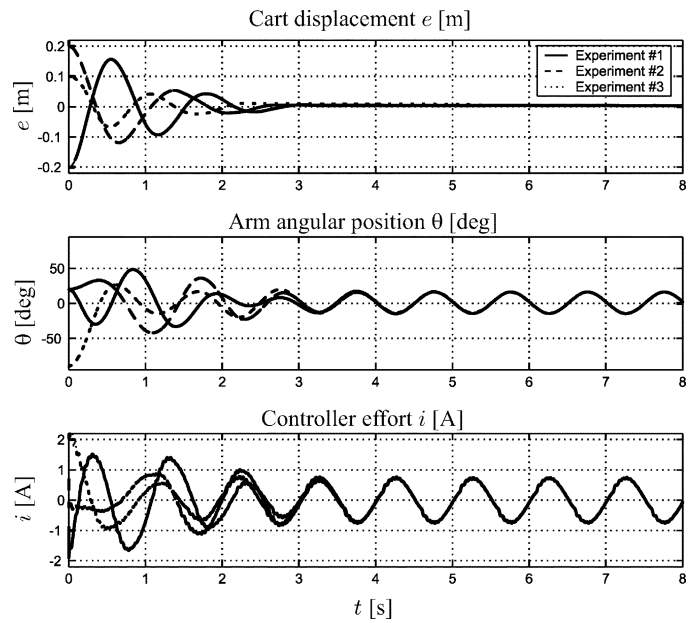

Fig. 8. Experiments for a disturbance force of amplitude $\mathcal{A} = 15$ N and predefined initial conditions.

In the experiments, the frequency of the disturbance force $F_d(t)$ (the frequency of the exosystem) is set to 1 Hz, which corresponds to ω in the exosystem (2) equal to $\omega = 2\pi$ rad/s.

The controller is implemented in the dSpace-system with the sampling frequency 4 kHz.

B. Experimental Results

All experiments are performed for the initial conditions of the exosystem equal to $w_1(0) = 0$, $w_2(0) = \mathcal{A}$. These initial conditions correspond to the disturbance force $F_d(t) := \mathcal{A}\sin(\omega t)$. We perform the experiments for two values of the amplitude $\mathcal{A}$: $\mathcal{A} = 15$ and $\mathcal{A} = 25$ N.

Two types of experiments are performed. In the experiments of the first type, the system starts in a given initial condition $e(0) = e_0$ [m], $\dot{e}(0) = 0$ m/s, $\theta(0) = \theta_0^\circ$, $\dot{\theta}(0) = 0\ ^\circ/$s. For each value of the amplitude $\mathcal{A}$, we perform three experiments corresponding to different initial conditions e_0 and θ_0. These initial conditions are given in Table I.

The results of the experiments corresponding to the disturbance amplitudes $\mathcal{A} = 15$ and $\mathcal{A} = 25$ N are presented in Figs. 8 and 9, respectively. In these figures, the controller effort is represented by the current $i = \kappa_A u_T$ A fed by the amplifier to the dc motor.

In the experiments of the second type, the system is affected once again by a disturbance force $F_d(t)$ of amplitude $\mathcal{A}$. Initially, only the feedback part in the controller (4) is active, i.e.,

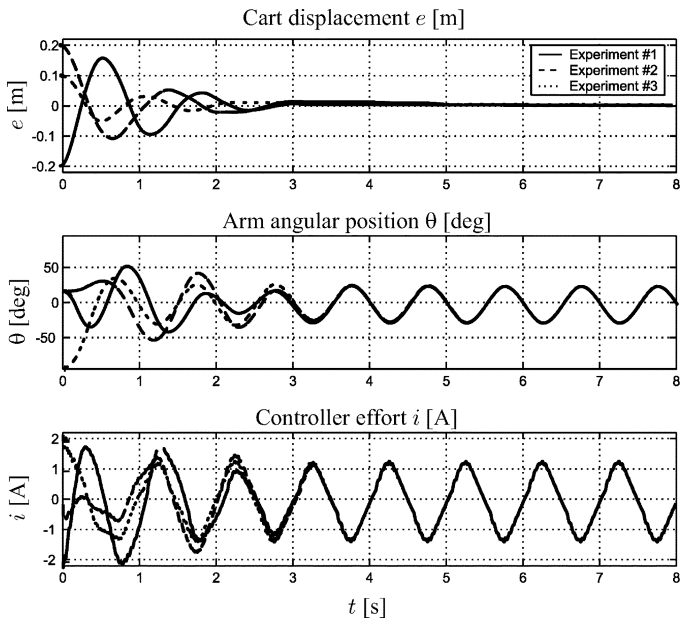

Fig. 9. Experiments for a disturbance force of amplitude $\mathcal{A} = 25$ N and predefined initial conditions.

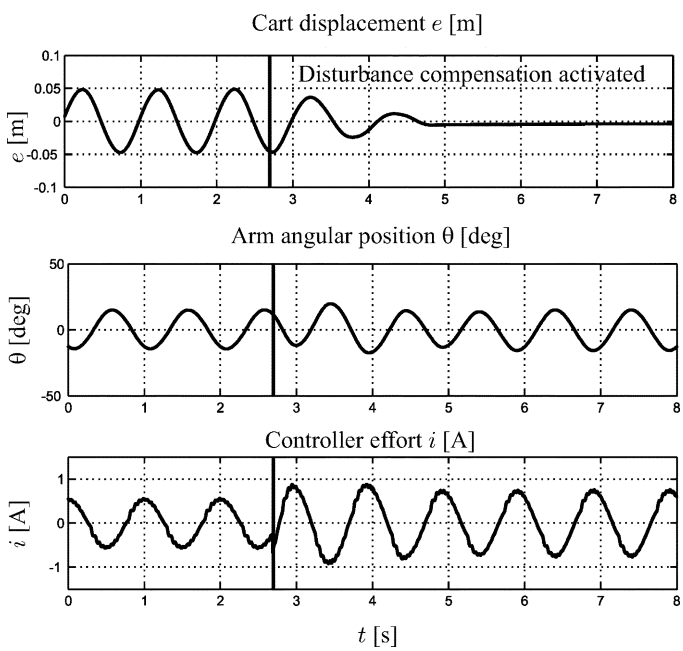

Fig. 10. Experiments for a disturbance force of amplitude $\mathcal{A} = 15$ N. Disturbance compensation is activated during the experiment.

$T_u = Kx$, and there is no compensation for the disturbance force $F_d(t)$. Since there is no disturbance compensation, the cart starts oscillating. At an arbitrary time instant t_* the feedforward part of the controller is activated, i.e., $T_u = c(w) + K(x - \pi(w))$. This results in disturbance rejection in the position of the cart e. The results of the experiments corresponding to the disturbance amplitudes $\mathcal{A} = 15$ and 25 N are presented in Figs. 10 and 11, respectively.

From these experimental results, we can immediately draw the following conclusion. The output regulation controller (4) does compensate a significant part of the harmonic disturbance

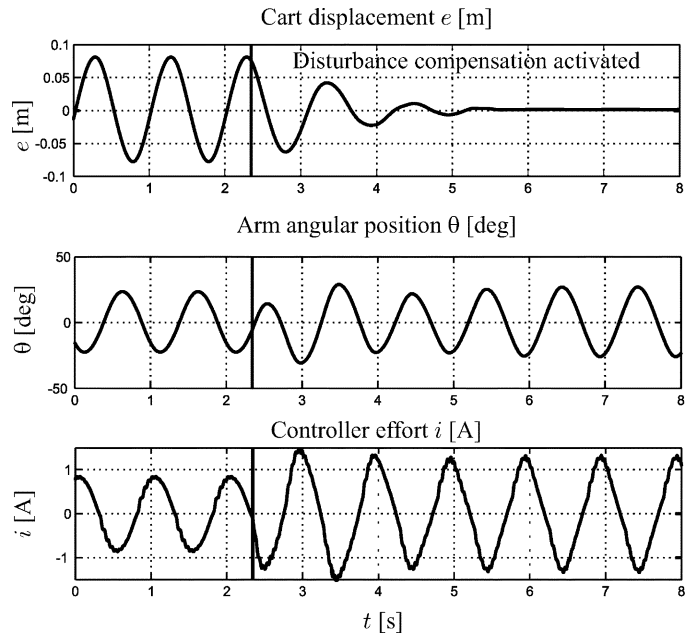

Fig. 11. Experiments for a disturbance force of amplitude $\mathcal{A} = 25$ N. Disturbance compensation is activated during the experiment.

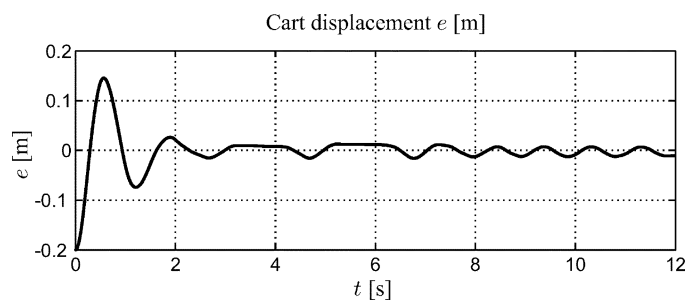

Fig. 12. Limit cycling in the cart motion. The disturbance force amplitude is $\mathcal{A} = 15$ N.

force acting on the cart. The residual friction in the cart motion manifests itself in the sticking phenomenon: after transients the cart stabilizes at an equilibrium position which is not equal to zero.

In Fig. 12, the cart displacement signal related to an experiment, performed at a different time, is depicted. Clearly, exact output regulation is not attained and a limit cycle of small amplitude remains. In this respect, it should be noted that the friction characteristics in the setup are subject to change due to temperature and humidity change in the laboratory. However, exactly the same friction compensation as in the previous experiments was used. Consequently, the limit cycling can be caused by an interaction of several factors: friction and friction compensation in the cart motion, friction and friction compensation in the rotating arm, and feedback controller and backlash in the gearhead. These problems require an additional investigation which is outside the scope of our research.

VI. Conclusion

In this brief, we have presented experimental results on the local output regulation problem for the TORA system. First, we have constructed a simple state-feedback controller which

solves a disturbance rejection problem for the TORA system. This problem is a particular case of the local output regulation problem. In order to validate this controller in experiments, an experimental setup for the TORA system has been built from an existing H-bridge setup. The proposed state-feedback controller has been implemented in this setup and tested in a row of experiments.

As follows from the results of these experiments, for the setup in closed-loop with the proposed controller output regulation only approximately occurs. This means that the regulated output $e(t)$ does not exactly tend to zero, but either sticks in an equilibrium position close to zero, or keeps on oscillating with a small amplitude. These phenomena are due to nonexact compensation of the friction and due to the backlash problem in the gearhead of the rotating arm. At the stage of controller design for the output regulation problem, these factors have not been taken into account.

In practice, there is always some type of (non) parametric uncertainty present in the system. It can be either due to inaccurately identified parameters of the system or due to friction, backlash, or other parasitic phenomena acting on the system, which are not taken into account in the system model. These uncertainties may significantly reduce the performance of a controller. This performance deterioration may manifest itself, for example, in a (large) steady-state regulation error, as illustrated by the experimental results on the TORA system previously presented. As follows from the experiments on the TORA system performed for different values of the controller gain K (these results are omitted here due to space limitations) this steady-state regulation error can be reduced by a proper choice of the gain K. Also, this gain matrix K essentially determines the region of admissible initial conditions for which this local controller works. Moreover, it determines the rate of convergence for the closed-loop system. In this brief, the choice of the matrix K, which takes into account these practically important design issues, is based on control engineering judgement. It should be noted that the problem of tuning controller parameters in a systematic way taking into account the previously mentioned design issues has not been considered in the literature on the output regulation problem so far. This fact urges the need for further work in this direction.

The results presented in this brief are the first steps in the field of experimental output regulation for nonlinear systems. Even with the *ad hoc* tuning of the controller gains and with many uncertainties present in the system, these results show relatively good performance of the closed-loop system. These successful experiments indicate that the output regulation theory can be successfully applied in experiments. Further work is under way to implement an output-feedback controller for the disturbance rejection problem considered in this brief and to reduce the sticking and limit cycling phenomena caused by friction and backlash.

REFERENCES

[1] B. Francis and W. Wonham, "The internal model principle of control theory," *Automatica*, vol. 12, pp. 457–465, 1976.

[2] E. Davison, "Multivariable tuning regulators: the feedforward and robust control of a general servomechanism problem," *IEEE Trans. Autom. Control*, vol. AC-21, no. 1, pp. 35–47, Jan. 1976.

[3] A. Isidori and C. Byrnes, "Output regulation of nonlinear systems," *IEEE Trans. Autom. Control*, vol. 35, no. 2, pp. 131–140, Feb. 1990.

[4] J. Huang and W. Rugh, "On a nonlinear multivariable servomechanism problem," *Automatica*, vol. 26, no. 6, pp. 963–972, 1990.

[5] C. Byrnes and A. Isidori, "Output regulation for nonlinear systems: An overview," *Int. J. Robust Nonlinear Control*, vol. 10, pp. 323–337, 2000.

[6] C. Byrnes, F. D. Priscoli, and A. Isidori, *Output Regulation of Uncertain Nonlinear Systems*. Boston, MA: Birkhäuser, 1997.

[7] A. Isidori, L. Marconi, and A. Serrani, *Robust Autonomous Guidance*. London, U.K.: Springer, 2003.

[8] J. Huang, *Nonlinear Output Regulation. Theory and Applications*. Philadelphia, PA: SIAM, 2004.

[9] A. Pavlov, N. van de Wouw, and H. Nijmeijer, *Uniform Output Regulation of Nonlinear Systems; A Convergent Dynamics Approach*. Boston, MA: Birkhäuser, 2005.

[10] A. Isidori, L. Marconi, and A. Serrani, "Autonomous vertical landing on an oscillating platform: an internal-model based approach," *Automatica*, vol. 38, no. 1, pp. 21–32, 2001.

[11] ——, "Robust nonlinear motion control of a helicopter," *IEEE Trans. Autom. Control*, vol. 48, no. 3, pp. 413–426, Mar. 2003.

[12] J. Huang and G. Hu, "A control design for the nonlinear benchmark problem via the output regulation method," *J. Control Theory Appl.*, vol. 2, no. 1, pp. 11–19, 2004.

[13] B. Vazquez, G. Silva, and J. Alvarez, "A nonlinear vibration absorber based on nonlinear control methods," in *Proc. 25th Int. Conf. Modal Analysis: Noise Vibration Eng.*, 2000, pp. 147–153.

[14] ——, "Active vibration control of an oscillating rigid bar using nonlinear output regulation techniques," in *Proc. SPIE 7th Int. Symp. Smart Structures Mater.*, 2000, pp. 368–376.

[15] C. Bonivento, A. Isidori, L. Marconi, and A. Paoli, "Implicit fault-tolerant control: Application to induction motors," *Automatica*, vol. 40, no. 3, pp. 355–371, 2004.

[16] Z. Lin, M. Glauser, T. Hu, and P. E. Allaire, "Magnetically suspended balance beam with disturbances: A test rig for nonlinear output regulation," in *Proc. IEEE Conf. Decision Control*, 2004, pp. 4577–4582.

[17] C.-J. Wan, D. Bernstein, and V. Coppola, "Global stabilization of the oscillating eccentric rotor," in *Proc. IEEE Conf. Decision Control*, 1994, pp. 4024–4029.

[18] Z.-P. Jiang and I. Kanellakopoulos, "Global output-feedback tracking for a benchmark nonlinear system," *IEEE Trans. Autom. Control*, vol. 45, no. 5, pp. 1023–1027, May 2000.

[19] M. Jankovic, D. Fontaine, and P. Kokotovic, "TORA example: Cascade- and passivity-based control designs," *IEEE Trans. Control Syst. Technol.*, vol. 4, no. 3, pp. 292–297, May 1996.

[20] A. Pavlov, N. van de Wouw, and H. Nijmeijer, "The local output regulation problem: Convergence region estimates," *IEEE Trans. Autom. Control*, vol. 49, no. 5, pp. 814–819, May 2004.

[21] A. Pavlov, N. van de Wouw, and H. Nijmeijer, "The local output regulation problem: Convergence region estimates," presented at the Eur. Control Conf., Cambridge, U.K., 2003.

[22] A. Pavlov, B. Janssen, N. van de Wouw, and H. Nijmeijer, "Experimental output regulation for the TORA system," in *Proc. IEEE Conf. Decision Control*, 2005, pp. 1108–1113.

[23] A. Isidori, *Nonlinear Control Systems*, 3rd ed. London, U.K.: Springer-Verlag, 1995.

[24] R. Hensen, "Controlled mechanical systems with friction," Ph.D. dissertation, Dept. Mech. Eng., Eindhoven Univ. Technol., Eindhoven, The Netherlands, 2002.

[25] B. Janssen, "Output regulation for a benchmark mechanical system: From design to experiments," M.S. thesis, Dept. Mech. Eng., Eindhoven Univ. Technol., Eindhoven, The Netherlands, 2005.

[26] A. Pavlov, N. van de Wouw, and H. Nijmeijer, "The local approximate output regulation problem: Convergence region estimates," *Int. J. Robust Nonlinear Control*, vol. 15, pp. 1–13, 2005.

[27] A. Pavlov, "The output regulation problem: A convergent dynamics approach," Ph.D. dissertation, Dept. Mech. Eng., Eindhoven Univ. Technol., Eindhoven, The Netherlands, 2004.

[28] D. Putra, "Control of limit cycling in frictional mechanical systems," Ph.D. dissertation, Dept. Mech. Eng., Eindhoven Univ. Technol., Eindhoven, The Netherlands, 2004.